

ALMA observations of a metal-rich damped Ly α absorber at $z = 2.5832$: evidence for strong galactic winds in a galaxy group[★]

J. P. U. Fynbo,^{1,2} K. E. Heintz,^{1,2,3} M. Neeleman,⁴ L. Christensen,²
M. Dessauges-Zavadsky,⁵ N. Kanekar,⁶ P. Møller,⁷ J. X. Prochaska,⁸ N. H. P. Rhodin,²
M. Zwaan⁷

¹The Cosmic Dawn Center, Niels Bohr Institute, University of Copenhagen, Juliane Maries Vej 30, 2100 Copenhagen Ø, Denmark

²Dark Cosmology Centre, Niels Bohr Institute, University of Copenhagen, Juliane Maries Vej 30, 2100 Copenhagen Ø, Denmark

³Centre for Astrophysics and Cosmology, Science Institute, University of Iceland, Dunhagi 5, 107 Reykjavík, Iceland

⁴Max-Planck-Institut für Astronomie, Königstuhl 17, D-69117, Heidelberg, Germany

⁵Observatoire de Genève, Université de Genève, 51 Ch. des Maillettes, 1290 Versoix, Switzerland

⁶Swarnajayanti Fellow; National Centre for Radio Astrophysics, Tata Institute of Fundamental Research, Pune 411007, India

⁷European Southern Observatory, Karl-Schwarzschild Strasse 2, D-85748 Garching, Germany

Accepted 2018 May 29. Received 2018 May 28; in original form 2018 May 1.

ABSTRACT

We report on the results of a search for CO(3-2) emission from the galaxy counterpart of a high-metallicity Damped Ly α Absorber (DLA) at $z = 2.5832$ towards the quasar Q0918+1636. We do not detect CO emission from the previously identified DLA galaxy counterpart. The limit we infer on M_{gas}/M_{\star} is in the low end of the range found for DLA galaxies, but is still consistent with what is found for other star-forming galaxies at similar redshifts. Instead we detect CO(3-2) emission from another intensely star-forming galaxy at an impact parameter of 117 kpc from the line-of-sight to the quasar and 131 km s⁻¹ redshifted relative to the velocity centroid of the DLA in the quasar spectrum. In the velocity profile of the low- and high-ionisation absorption lines of the DLA there is an absorption component consistent with the redshift of this CO-emitting galaxy. It is plausible that this component is physically associated with a strong outflow in the plane of the sky from the CO-emitting galaxy. If true, this would be further evidence, in addition to what is already known from studies of Lyman-break galaxies, that galactic outflows can be traced beyond 100 kpc from star-forming galaxies. The case of this $z = 2.583$ structure is an illustration of this in a group environment.

Key words: galaxies: ISM – ISM: molecules – quasar: absorption lines – quasars: individual (Q 0918+1636) – submillimeter: ISM

1 INTRODUCTION

The most hydrogen rich class of quasar absorption systems, the DLAs (defined to have $N(\text{H I}) \geq 2 \times 10^{20}$ cm⁻², Wolfe et al. 2005), remain one of the most compelling ways to probe the properties of galaxies, in particular at redshifts 2 – 5 (see Wolfe et al. 2005, for a review). This class of absorbers gives access to detailed information about chemical evolution. The technique is obviously limited to gas-rich galaxies, but is otherwise not limited to only the brightest galaxies as most other techniques are (Fynbo et al. 2008).

Early on in the studies of DLAs, it was realized that it is important to determine the emission properties of the DLAs in order to connect the information collected from absorption studies with the rapidly growing body of information on high- z galaxies based on emission studies. The Atacama Large Millimeter/sub-millimeter Array, ALMA, has opened up a new possibility to do this at sub-

★ This paper makes use of the following ALMA data: ADS/JAO.ALMA#2016.1.00628.S (PI Prochaska). ALMA is a partnership of ESO (representing its member states), NSF (USA) and NINS (Japan), together with NRC (Canada) and NSC and ASIAA (Taiwan) and KASI (Republic of Korea), in cooperation with the Republic of Chile. The Joint ALMA Observatory is operated by ESO, AUI/NRAO and NAOJ. Based on observations made with the Nordic Optical Telescope, operated by the Nordic Optical Telescope Scientific Association at the Observatorio del Roque de los Muchachos, La Palma, Spain, of the Instituto de Astrofísica de Canarias. Based on observations made with the NASA/ESA Hubble Space Telescope, obtained at the Space Telescope Science Institute (STScI), which is operated by the Association of Universities for Research in Astronomy, Inc., under NASA contract NAS 5-26555. These observations are associated with programme 12553.

millimeter wavelengths. An advantage of this approach is that the contrast between the bright background quasar and the faint DLA galaxy at these wavelengths typically is much smaller than in the optical or near-IR bands. The first pilot studies of DLAs with ALMA have given quite interesting results. Møller et al. (2018) studied a single system at $z = 0.716$ and found a surprisingly large molecular mass and for that mass surprisingly low star-formation rate placing the object away from the normal galactic scaling relations for these quantities. Kanekar et al. (2018) studied a sample of DLAs at similar redshifts and found a surprisingly large detection rate of CO-emission from the galaxy counterparts of the absorbers. The first reported detection of CO-emission from a study targeting the field of a $z > 2$ DLA is that of Neeleman et al. (2018). In the field of the $z = 2.19289$ DLA towards QSO B1228-113 they detected a strong CO-emitter $3.7''$ (30 kpc) from the quasar sightline.

In this paper we present new observations of the field of the $z = 2.5832$ DLA absorber towards Q0918+1636, which has already been studied in substantial detail using both imaging and spectroscopy in optical to near-infrared wavebands. The DLA has a high gas-phase metallicity with measured abundances of $[\text{Zn}/\text{H}] = -0.12 \pm 0.05$ and $[\text{S}/\text{H}] = -0.26 \pm 0.05$. The system also shows absorption features from H_2 molecules with a column density within the range of $N(\text{H}_2) = 1.5 \times 10^{16} - 1.1 \times 10^{19} \text{ cm}^{-2}$ (the large uncertainty reflecting that the individual absorption components of the H_2 lines are not resolved in the X-shooter spectrum). The galaxy counterpart is detected at a projected distance of 1.98 arcsec from the quasar (i.e. 16.2 kpc at $z = 2.5832$). The optical emission lines from $[\text{O II}]$, $[\text{O III}]$, $\text{H}\beta$ and $\text{H}\alpha$ are seen in the combined X-shooter spectrum, and using emission line diagnostics, Fynbo et al. (2013, hereafter F13) found a metallicity of $12 + \log(\text{O}/\text{H}) = 8.8 \pm 0.2$ ($[\text{X}/\text{H}]_{\text{em}} = 0.11 \pm 0.20$), consistent with that inferred in absorption (up to the uncertainties that remain on the absolute calibration of emission line metallicity diagnostics). The difference between the absorption and emission redshift amounts to only $36 \pm 20 \text{ km s}^{-1}$ (F13). From an Spectral Energy Distribution (SED) fit to the optical and near-IR photometric data, F13 derived a stellar mass of $\log(M_*/M_\odot) = 10.10^{+0.17}_{-0.11}$ and a star-formation rate (SFR) of $27^{+20}_{-9} M_\odot \text{ yr}^{-1}$ for the DLA emission counterpart. In addition, the SED fit infers a dust attenuation of $A_V = 1.54^{+0.72}_{-0.56}$ mag. These properties made the system a promising target for our ALMA study of metal-rich DLAs at $z \gtrsim 2$ (Neeleman et al. 2018). In this paper we present ALMA observations of the field targeting the CO(3–2) line.

We assume a standard flat cosmology with $H_0 = 67.8 \text{ km s}^{-1} \text{ Mpc}^{-1}$, $\Omega_m = 0.308$ and $\Omega_\Lambda = 0.692$ (Planck Collaboration et al. 2016).

2 ALMA OBSERVATIONS

The field surrounding Q0918+1636 was observed with ALMA on UT 2017 January 9 with a compact configuration (maximum baseline of 383 m) for a total on-source integration time of 2117 seconds. Quasar J0852+2006 was used for bandpass and phase calibration, and quasar J0750+1231 was used for flux calibration. The local oscillator was tuned so one of the four spectral windows was centered on the redshifted CO(3–2) line at 96.5 GHz with a frequency resolution of 3.9 MHz. The remaining three spectral windows were set up to measure continuum emission of the field.

The initial data were calibrated using the ALMA pipeline, which is part of the Common Astronomy Software Applications (CASA; McMullin et al. 2007) package. After this initial round

of calibration, additional flagging was performed in CASA. The continuum image was generated from the three continuum spectral windows, using natural weighting, resulting in a synthesized beam of $3.''2 \times 2.''5$ at 69° . The resulting root mean square (RMS) noise of the continuum image is $14.3 \mu\text{Jy beam}^{-1}$, no sources were detected in this image at high signal-to-noise ($S/N > 5\sigma$).

Using the task TCLEAN in CASA, a spectral cube was made from the spectral window centered on the CO(3–2) emission at the redshift of the $z = 2.5832$ DLA. Natural weighting was used and the cube was Hanning-smoothed to a velocity resolution of 48.5 km s^{-1} , resulting in a RMS noise of $0.24 \text{ mJy beam}^{-1}$ per 48.5 km s^{-1} channel. The spectral cube spans a velocity window of $\pm 2890 \text{ km s}^{-1}$ around the DLA redshift.

3 RESULTS

The full ALMA spectral cube was searched for line emission. Only a single line source was detected at a $S/N > 7$. We do detect one other possible line emission line at 5.8σ centered at -700 km s^{-1} and $35''$ south-west of the quasar, but no optical counterpart in the *HST* imaging is seen at this position. Assuming Gaussian noise characteristics, the chance probability of such a signal to occur in the full data cube due to noise fluctuations is 7×10^{-4} . We note that the signal is detected at $> 4\sigma$ in two consecutive, independent (24 km s^{-1}) channels, suggesting the emission is real. However, without a clear optical counterpart, it is hard to interpret this tentative detection.

3.1 Limit on CO emission from the DLA galaxy counterpart

At the location of the previously identified DLA galaxy counterpart—2 arcsec west of the quasar—no emission was seen in either the spectral cube or continuum emission. In the top panel of Fig. 2 we show the ALMA spectrum around the expected position of the CO(3–2) line. The 1σ RMS noise for a 100 km s^{-1} channel is 0.167 mJy/beam . Assuming a similar line width for the emission profile gives a 3σ upper limit on the velocity-integrated line flux of $0.050 \times (\Delta V / 100 \text{ km s}^{-1})^{1/2} \text{ Jy km s}^{-1}$. At $z = 2.5832$ this corresponds to a line luminosity of $L'_{\text{CO}(3-2)} < 1.7 \times 10^9 \text{ K km s}^{-1} \text{ pc}^2$, using the conversion formula from Solomon & Vanden Bout (2005). To estimate the molecular mass, we assume $L'_{\text{CO}(3-2)}/L'_{\text{CO}(1-0)} = 0.57$ (Dessauges-Zavadsky et al. 2015), and a CO-to- H_2 conversion of $\alpha_{\text{CO}} = 4.3 M_\odot (\text{K km s}^{-1} \text{ pc}^2)^{-1}$ (Bolatto et al. 2013), which results in an upper limit on the molecular gas mass of $M_{\text{mol}} < 1.3 \times 10^{10} M_\odot$. Given the stellar mass of $M_* = 12.6^{+6.1}_{-2.9} \times 10^9 M_\odot$ (from F13) the ratio of M_{mol}/M_* is still consistent with the general redshift evolution of gas-to-stellar mass inferred from main-sequence galaxies (e.g., Magdis et al. 2012b).

For comparison, the $z \sim 0.7$ absorption-selected sample (Møller et al. 2018; Kanekar et al. 2018; Klitsch et al. 2018) have measured molecular masses ranging between $0.6 - 8.2 \times 10^{10} M_\odot$, with two non-detections below a molecular mass of $5 \times 10^9 M_\odot$. In addition, the molecular mass of a $z = 0.101$ galaxy-absorber pair is $M_{\text{mol}} = (4.2 \pm 0.2) \times 10^9 M_\odot$ (Neeleman et al. 2016) and the galaxy associated with a $z = 2.193$ DLA discussed in Neeleman et al. (2018) has a molecular mass of $(1.4 \pm 0.2) \times 10^{11} M_\odot$.

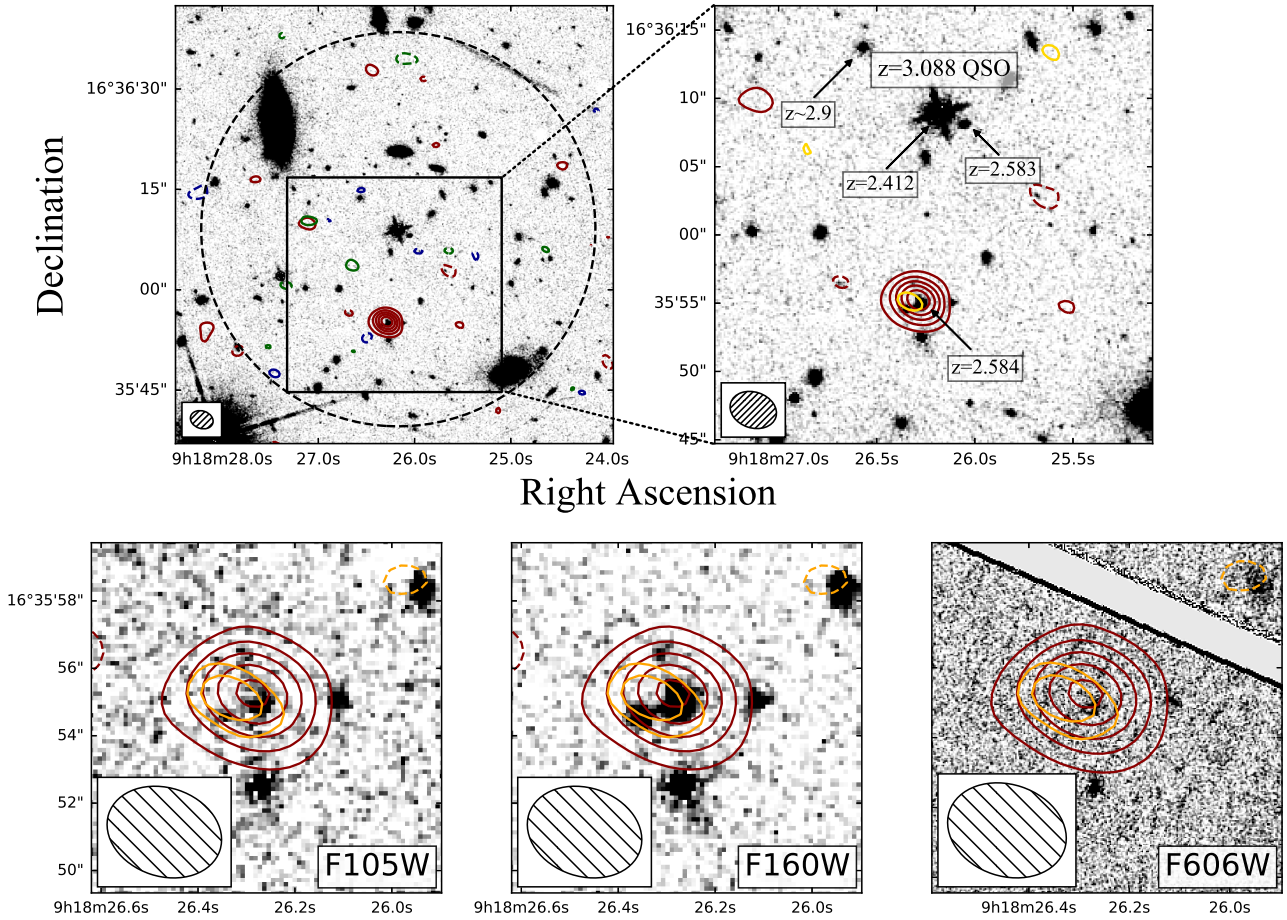


Figure 1. Top panels: Integrated CO(3–2) emission (red contours) and dust continuum (yellow contours) overlaid on the HST/F160W image. The left panel shows the full field of view of the ALMA observation and the right panel a zoom on the region around the quasar. No CO emission is detected down to $0.050 \times (\Delta V / 100 \text{ km s}^{-1})^{1/2} \text{ Jy km s}^{-1}$ at the position of the previously identified galaxy counterpart 2 arcsec west of the quasar. The CO-emitting galaxy is located at a projected distance of 14.2 arcsec (117 kpc at $z = 2.5832$) relative to the quasar. Bottom panels: Integrated CO(3–2) emission (red contours) and dust continuum (orange contours) overlaid on the HST F606W, F105W and F160W images from F13 from the galaxy located at a distance of 14.2 arcsec (117 kpc at $z = 2.5832$) south of the quasar. The synthesized beam of the ALMA observation is shown in the lower left corner of each panel.

3.2 The CO-emitting galaxy at $\Delta v = 131 \text{ km s}^{-1}$

3.2.1 CO emission and molecular gas mass

While no CO(3–2) line emission is detected at the position of the previously identified DLA counterpart, we do detect a strong CO-emitting galaxy at a projected distance of 14.2 arcsec (117 physical kpc at $z = 2.5832$) south of the DLA (see Fig. 1). The galaxy is also tentatively detected in dust continuum, albeit at a lower signal-to-noise ratio, with a measured flux density of $40 \pm 13 \mu\text{Jy}$. The integrated CO(3–2) and dust continuum emission from the ALMA observations are shown in Fig. 1, overlaid on the *HST* images of the galaxy from F13.

In the *HST* F160W image there are multiple emission components near the position of the ALMA source. Unfortunately, the resolution of the spectral cube emission is insufficient to resolve the CO emission. Together with the known offset in absolute astrometry between ALMA and *HST* (e.g., Dunlop et al. 2017), we cannot establish if this is a chance projection of several galaxies at different redshift or emission from regions in the same galaxy. In the following, we will assume the latter. As Fig. 1 shows, the CO

emission is co-spatial with a very red component that is only seen in the F160W band.

From the CO spectral cube, we have extracted a line profile at the position of the CO emission, which is shown in the bottom panel in Fig. 2. The spectrum shows that the CO emission is redshifted from the centroid of the DLA at $z = 2.5832$ by 131 km s^{-1} . There is marginal evidence for a "boxy" or double-horned line profile (Davis et al. 2011), similar to the CO(2–1) and CO(1–0) line profiles observed for two other, low- z absorbing galaxies (Neeleman et al. 2016; Møller et al. 2018). This indicates that this galaxy has some degree of a rotational support and/or emission from several sub-clumps.

The velocity-integrated flux density of the CO(3–2) emission line is $0.73 \pm 0.08 \text{ Jy km s}^{-1}$. This corresponds to a luminosity of $L'_{\text{CO}(3-2)} = (2.5 \pm 0.3) \times 10^{10} \text{ K km s}^{-1} \text{ pc}^2$.

The star-formation rate of this galaxy (see Sect. 3.2.3) is similar to the galaxy discussed in Neeleman et al. (2018), where we assumed an $\alpha_{\text{CO}} = 4.3 M_{\odot} (\text{K km s}^{-1} \text{ pc}^2)^{-1}$ conversion factor and $L'_{\text{CO}(3-2)}/L'_{\text{CO}(1-0)} = 0.57$. To facilitate comparison, we will use similar values here, although recent work suggest some

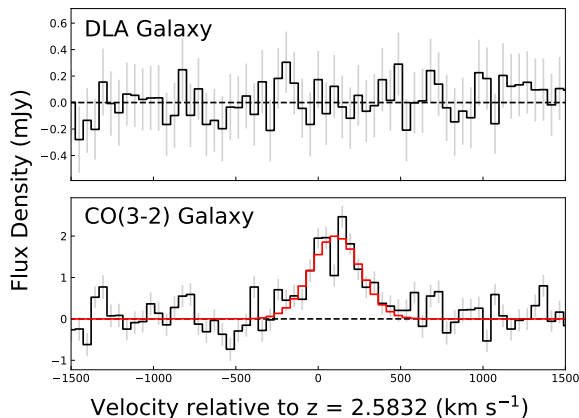


Figure 2. CO flux density as a function of velocity, where $v_{\text{rel}} = 0 \text{ km s}^{-1}$ corresponds to $z_{\text{DLA}} = 2.5832$. The top panel shows the non-detection of the DLA galaxy and the bottom panel the spectrum of the CO galaxy 117 kpc from the quasar sightline. A simple Gaussian profile is fit to the data with an offset of $\delta v = 131 \text{ km s}^{-1}$ relative to z_{DLA} .

absorption-selected galaxies might show more starburst-like interstellar medium conditions (Klitsch et al. 2018). To account for this uncertainty, the lower uncertainty on the mass includes the assumption of starburst-like conditions. Using these conversion factors then yields a molecular gas mass of $M_{\text{mol}} = (1.8^{+0.2}_{-1.6}) \times 10^{11} M_{\odot}$.

3.2.2 Associated absorption at the CO galaxy redshift in the quasar spectrum

In Fig. 3 we show the normalized quasar spectrum in regions around selected low- and high-ionisation metal lines from the $z = 2.5832$ DLA. A weak absorption feature is visible at $\Delta v = 131 \text{ km s}^{-1}$ in the low-ionisation lines and in the high-ionisation lines there is quite strong absorption.

C IV and Si IV absorption indicates the presence of a warm-hot plasma in galaxy halos or in the IGM and is observed in most quasar and GRB-DLAs (e.g. Fox et al. 2008, 2009, and Heintz et al., submitted). The large extent of the C IV and Si IV absorption line profiles are therefore expected since this gas traces a more extended medium than the galaxy ISM. In Fig. 3 we also look for extended Mg II absorption due to the large stellar mass of the CO-emitting galaxy (see Sect. 3.2.3 below) since the extent of the Mg II absorbing gas is found to scale with stellar mass and specific star-formation rate (Chen et al. 2010). We do also see extended absorption in the region of Mg II $\lambda\lambda 2796, 2803$ (albeit in a spectral region in the near-IR affected by strong emission lines from airglow). There is also indications of absorption from N V and O VI in the spectrum, but both features are heavily blended. It is intriguing that the high-ionisation metal lines might originate in the IGM between a group of galaxies at $z = 2.5832$.

We also note that the H₂ absorption in the quasar spectrum is distributed over about 55 km^{-1} in velocity space centred around the mean peak of low-ionisation absorption (see the lower panel in Fig. 4 in Fynbo et al. 2011). Hence, the H₂ absorption is most likely associated with gas originating in the DLA galaxy counterpart 16 kpc from the quasar.

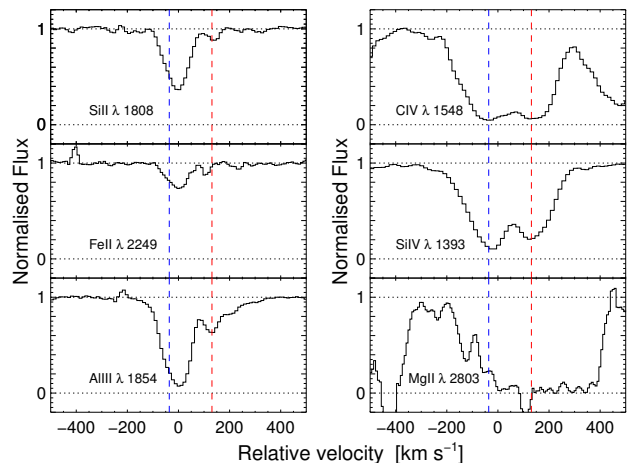


Figure 3. Sections from the normalized X-shooter spectrum of Q0918+1636 around selected low- and high-ionisation absorption lines from the DLA. The zero-point of the velocity is set to $z_{\text{DLA}} = 2.5832$. The blue dashed line marks the redshift of the previously identified galaxy counterpart at an impact parameter of 16.2 kpc. The red dashed line marks the velocity offset of 131 km s^{-1} measured from the centroid of the CO(3-2) emission line from the galaxy 117 kpc from the quasar.

Table 1. Photometric data for the three galaxies in the field at $z \approx 2.5$ (using a 2 arcsec diameter circular aperture). Magnitudes for the DLA galaxy are from F13. All magnitudes are given in the AB system and are not corrected for the Galactic reddening of $E(B-V) = 0.022 \text{ mag}$ (Schlafly & Finkbeiner 2011).

Band	Source		
	DLA galaxy	CO galaxy	Gal. at $z_{\text{phot}} = 2.9^{+0.4}_{-0.9}$
<i>F606W</i>	25.46 ± 0.13	26.59 ± 0.25	27.56 ± 0.19
<i>F105W</i>	24.62 ± 0.09	24.70 ± 0.13	25.34 ± 0.15
<i>F160W</i>	23.68 ± 0.06	23.63 ± 0.07	23.48 ± 0.07
<i>u</i>	$> 26.5 (3\sigma)$	$> 26.5 (3\sigma)$	$> 26.5 (3\sigma)$
<i>g</i>	25.9 ± 0.3	$> 26.2 (3\sigma)$	$> 26.2 (3\sigma)$
<i>K_s</i>	$> 23.3 (3\sigma)$	$> 23.3 (3\sigma)$	$> 23.3 (3\sigma)$

3.2.3 Physical properties from SED fitting

The field of Q0918+1636 has been observed with the Wide Field Camera 3 (WFC3) on-board *HST* in the *F606W*, *F105W*, and *F160W* filters, and with the Andalucia Faint Object Spectrograph and Camera (ALFOSC) and the Nordic Optical Telescope near-infrared Camera and spectrograph (NOTCam) at the NOT (see F13 for details). From the NOT we obtained *u* and *g* SDSS filter images using ALFOSC and a *K_s* band image using NOTCam. Using these imaging data we measure the magnitudes in circular apertures with a diameter of 2 arcsec for the CO galaxy and report them in Table 1. For comparison we also list the magnitudes for the DLA emission counterpart (from F13) and for a galaxy that has been photometrically determined to be possibly located at a similar redshift (see Sect. 3.3 below). This galaxy is not detected in the ALMA data.

To determine the physical properties of the CO-emitting

Table 2. Physical properties of the CO galaxy from SED fitting and from the ALMA observations.

Parameter	Value
Age (Myr)	217^{+341}_{-137}
A_V (mag)	$1.88^{+0.50}_{-0.50}$
SFR ($M_\odot \text{ yr}^{-1}$)	112^{+111}_{-68}
$\log(M_\star/M_\odot)$	$10.45^{+0.10}_{-0.20}$
$\log(L_{\text{dust}}/L_\odot)$	$12.05^{+0.30}_{-0.30}$
$\log(M_{\text{dust}}/M_\odot)$	$7.95^{+0.20}_{-0.30}$
$\log(M_{\text{mol}}/M_\odot)$	$11.26^{+0.04}_{-0.95}$

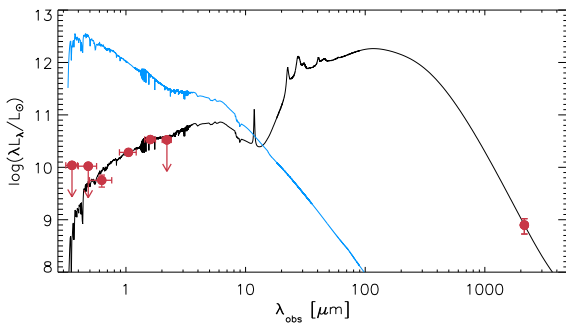


Figure 4. The broad-band optical to near-infrared SED of the CO-emitting galaxy. The red points denotes the measured photometric data points and upper limits (arrows). From blue to red wavelengths: ALFOSC u and g bands, *HST*/WFC3 $F606W$, $F105W$ and $F160W$ bands, the NOTCam K_s band, and the ALMA continuum detection. The best-fit galaxy model is shown as the black line. The stellar component without dust-extinction is shown with a blue line.

galaxy we use MAGPHYS¹ (da Cunha et al. 2008), with the photometry in Table 1 but corrected for the Galactic foreground extinction of $E(B - V) = 0.022$ mag (Schlafly & Finkbeiner 2011). MAGPHYS is a tool that fits the photometric data to stellar population and dust emission synthesis models, assuming a Chabrier (2003) IMF to generate the output galaxy models. We also include the detection of the continuum flux determined from the ALMA data. The results of the spectral energy distribution (SED) fits are provided in Table 2 and the generated galaxy model is illustrated in Fig. 4. The age, extinction and stellar mass of the CO-emitting galaxy are all similar with those inferred for the DLA galaxy. The SFR, however, is almost an order of magnitude higher than that of the DLA galaxy. We stress that this photometric modeling is only the best possible with the data in hand. Looking at the morphology of the object it clearly consists of multiple components with different colours so likely both age, the SFR and the dust vary across the object.

3.3 Galaxies in the field around Q 0918+1636

In order to search for other possible members of the $z = 2.5832$ structure revealed by the DLA and the CO galaxy we determine photometric redshift measurements of galaxies in the overlapping

¹ <http://www.iap.fr/magphys/>

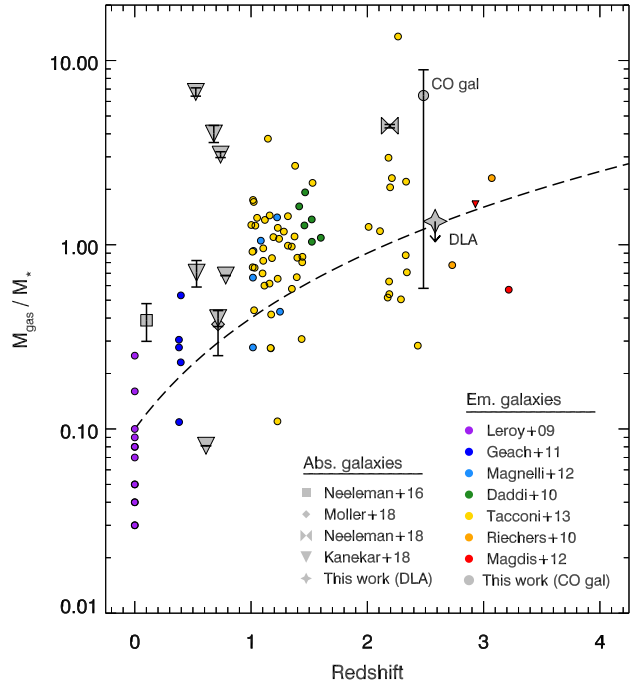


Figure 5. The ratio of gas mass to stellar mass as a function of redshift for various emission (small circles) and absorption selected galaxy samples (gray symbols). The upper limit for the DLA counterpart and the detection for the CO-emitting galaxy in the Q0918+1636 field are the two gray symbols at $z = 2.583$ (the point for the CO-galaxy has been shifted slightly to the left to increase visibility). For both the DLA counterpart and the CO-galaxy we show M_{gas}/M_\star assuming $\alpha_{\text{CO}} = 4.3$, but the error-bar includes the possibility for $\alpha_{\text{CO}} = 1$. The measurements from other star-forming galaxies are taken from Leroy et al. (2009); Geach et al. (2011); Magnelli et al. (2012); Daddi et al. (2010); Tacconi et al. (2010, 2013); Riechers et al. (2010), and Magdis et al. (2012a). The data for DLA galaxies are from Neeleman et al. (2016, 2018); Møller et al. (2018), and Kanekar et al. (2018). The dashed curve follows $M_{\text{gas}}/M_\star = 0.1 \times (1 + z)^2$ (e.g., Geach et al. 2011; Carilli & Walter 2013).

region of the *HST* and NOT imaging data. One additional object (marked with $z \sim 2.9$ in the upper left panel of Fig. 1, has a photometric redshift consistent with 2.6, but we need spectroscopic measurements to establish with certainty if this galaxy is really at the same precise redshift.

4 DISCUSSION

To place the measurements from the field of Q0918+1636 in context we show in Fig. 5 our molecular and stellar mass measurements in a plot showing the evolution of M_{gas}/M_\star as a function of redshift (following Carilli & Walter (2013)). For comparison, we show measurements from a range of studies of both starformation and absorption selected galaxies. The upper limit on the M_{gas}/M_\star ratio is in the low end of the range found for DLA galaxies, but is otherwise consistent with what has been found for star-forming galaxies in general. The non-detection of CO(3-2) emission is therefore not very surprising for the DLA and it seems that a detection will be possibly with a slightly fainter detection limit.

With the detection of the CO-emitting galaxy we can probe this $z = 2.5832$ structure at three locations and phases: the metal-

rich and H₂-bearing DLA in the quasar spectrum at $z = 2.5832$, the previously identified galaxy counterpart blueshifted by 35 km s^{-1} at an impact parameter of 16.2 kpc relative to the DLA and now the CO-emitting galaxy redshifted by 131 km s^{-1} at an impact parameter of 117 physical kpc from the DLA. Photometric redshifts indicate that there could be other luminous members of the group. There is evidence from the kinematics that a minor part of the low-ionisation absorption and a larger fraction of the high-ionisation absorption in the DLA could be caused by gas associated with the CO-emitting galaxy. Whereas we cannot rule out that the match is a chance effect, a causal relation seems plausible. The impact parameter of 117 kpc combined with the age of the star-burst as estimated from SED-fitting requires a galactic wind velocity of several hundred km s^{-1} , which is not unreasonable (e.g., Geach et al. 2014). Together, this shows that the system is a likely part of a galaxy group and the galactic winds from at least the two identified galaxies are enriching the group-environment with metals, neutral hydrogen, dust and molecules (see also Sommer-Larsen & Fynbo 2017).

High- z DLAs have previously been found in environments with other nearby galaxies (e.g., Macchetto et al. 1993; Møller & Warren 1993; Francis & Hewett 1993; Warren & Møller 1996; Møller & Warren 1998; Fynbo et al. 2003; Schulze et al. 2012). In the work of Møller & Warren (1993) and Warren & Møller (1996) a group of three galaxies were found within 20 arcsec corresponding to about 150 kpc from the quasar line-of-sight. In this case the DLA is a proximate DLA so the quasar itself should be included in the structure. The study of Fynbo et al. (2003) found a large pancake-like structure marked out by 23 Lyman- α emitters in the field of an intervening DLA at $z = 2.85$ towards Q2138–4427. There are also many examples of DLAs or Lyman-limit systems originating from galaxies in group environments at lower redshifts (Kacprzak et al. 2010; Christensen et al. 2014; Klitsch et al. 2018; Rahmani et al. 2018).

We know from a range of different other lines of research that galaxies must expel large amounts of metals into their environments. In clusters of galaxies the metals can be directly inferred from observations in the X-ray band of the intracluster medium (e.g., Arnaud et al. 1992; Renzini 1997). The evidence supports a scenario, in which the metals in the intracluster medium was expelled from galaxies at early times (e.g., Ettori 2005; Mantz et al. 2017). The extent of halos of high-ionisation gas has previously been explored for Lyman-break galaxies at redshifts of 2.5–3.5 (Adelberger et al. 2005). This study found that strongly star-forming galaxies, with typical star-formation rates of several tens of solar masses per year, are generally associated with haloes of ionised gas traced by C IV out to $\sim 80 \text{ kpc}$ for $N_{\text{C IV}} \gtrsim 10^{14} \text{ cm}^{-2}$. This work was extended by Steidel et al. (2010) who studied both high- and low-ionisation absorption lines traceable out to impact parameters of about 100 kpc from $z = 2 - 3$ Lyman-break galaxies. More recently, Bielby et al. (2017) also explored the correlation between Lyman-break galaxies and absorption from neutral hydrogen and again found a clear correlation with a clustering length of $270 \pm 140 \text{ kpc}$ for H I absorbers with column densities in the range $N_{\text{H I}} = 10^{14.5} - 10^{16.5} \text{ cm}^{-2}$. Finally we note that, the DLA studied by Neeleman et al. (2017) also shows evidence for a galactic wind given the large impact parameter of the identified galaxy counterpart (45 kpc) and a large velocity spreads in the low-ionization metal lines.

We know less about the presence of molecules in the circumgalactic medium at these redshifts. In the present case we know there is H₂ at $z = 2.5832$ at several velocity components along the line

of sight to the background quasar. We also now know that there is molecular gas in the star-burst galaxy 117 kpc from the quasar line of sight. An interesting local analogue is M82, from which Walter et al. (2002) detect molecular gas in the galactic wind more than a kpc away from the disk. At intermediate redshifts, Geach et al. (2014) have found a strong molecular outflow from a star-burst galaxy at $z = 0.7$ where molecular gas is distributed over more than 10 kpc from an otherwise very compact starburst. Ginolfi et al. (2017) discuss an even more extended molecular gas distribution around a massive star-forming galaxy at $z = 3.47$ extending over more than 40 kpc.

The fact that both the low- and high-ionisation lines in the quasar spectrum appear to have contributions from several galaxies, including some at impact parameters beyond 100 kpc, in a group environment may be part of the reason why simulations of DLA kinematics have had difficulties matching the large line-widths of DLAs (Prochaska & Wolfe 1997; Ledoux et al. 1998; Pontzen et al. 2008; Barnes & Haehnelt 2009; Bird et al. 2015). The relatively strong correlation between metallicity and absorption line widths (Ledoux et al. 2006; Møller et al. 2013; Neeleman et al. 2013; Christensen et al. 2014), may in addition to a mass-metallicity relation, also be partly influenced by the effect of environment: high metallicity systems will preferentially trace more biased regions of the Universe with a higher than average galactic density. We finally note that strong feedback, especially for halo masses in the range $10^{11} - 10^{12} h^{-1} M_{\odot}$ is required to match the column density distribution of DLAs (Bird et al. 2014).

4.1 Summary

In summary, we do not detect CO emission from the previously identified DLA galaxy counterpart. This non-detection is still consistent with the distribution of M_{gas}/M_{\star} found for other star-forming galaxies. Instead we detect CO(3-2) from another intensely star-forming galaxy at an impact parameter of 117 kpc from the line-of-sight to the quasar and 131 km s^{-1} redshifted relative to the velocity centroid of the DLA in the quasar spectrum. In the velocity profile of the low- and high-ionisation absorption lines of the DLA there is an absorption component consistent with the redshift of the CO-emitting galaxy. It is plausible that this component is physically associated with a strong outflow in the plane of the sky from the CO-emitting galaxy. If true, this would be further evidence, in addition to what is already known from studies of Lyman-break galaxies, of strong galactic outflows traceable to impact parameters of at least 100 kpc.

ACKNOWLEDGEMENTS

We thank the anonymous referee for a very constructive and helpful report. We thank Georgios Magdis for helpful discussions during the preparation of this manuscript. The Cosmic Dawn center is funded by the DNRF. KEH acknowledges support by a Project Grant (162948–051) from The Icelandic Research Fund. The National Radio Astronomy Observatory is a facility of the National Science Foundation operated under cooperative agreement by Associated Universities, Inc. LC and NHR are supported by DFF-4090-00079. MN acknowledges support from ERC Advanced Grant 740246 (Cosmic_Gas).

REFERENCES

- Adelberger K. L., Shapley A. E., Steidel C. C., Pettini M., Erb D. K., Reddy N. A., 2005, *ApJ*, **629**, 636
- Arnaud M., Rothenflug R., Boulade O., Vigroux L., Vangioni-Flam E., 1992, *A&A*, **254**, 49
- Barnes L. A., Haehnelt M. G., 2009, *MNRAS*, **397**, 511
- Bielby R. M., et al., 2017, *MNRAS*, **471**, 2174
- Bird S., Vogelsberger M., Haehnelt M., Sijacki D., Genel S., Torrey P., Springel V., Hernquist L., 2014, *MNRAS*, **445**, 2313
- Bird S., Haehnelt M., Neeleman M., Genel S., Vogelsberger M., Hernquist L., 2015, *MNRAS*, **447**, 1834
- Bolatto A. D., Wolfire M., Leroy A. K., 2013, *ARA&A*, **51**, 207
- Carilli C. L., Walter F., 2013, *ARA&A*, **51**, 105
- Chabrier G., 2003, *PASP*, **115**, 763
- Chen H.-W., Wild V., Tinker J. L., Gauthier J.-R., Helsby J. E., Shtetman S. A., Thompson I. B., 2010, *ApJ*, **724**, L176
- Christensen L., Møller P., Fynbo J. P. U., Zafar T., 2014, *MNRAS*, **445**, 225
- Daddi E., et al., 2010, *ApJ*, **713**, 686
- Davis T. A., et al., 2011, *MNRAS*, **414**, 968
- Dessauges-Zavadsky M., et al., 2015, *A&A*, **577**, A50
- Dunlop J. S., et al., 2017, *MNRAS*, **466**, 861
- Ettori S., 2005, *MNRAS*, **362**, 110
- Fox A. J., Ledoux C., Vreeswijk P. M., Smette A., Jaunsen A. O., 2008, *A&A*, **491**, 189
- Fox A. J., Prochaska J. X., Ledoux C., Petitjean P., Wolfe A. M., Srianand R., 2009, *A&A*, **503**, 731
- Francis P. J., Hewett P. C., 1993, *AJ*, **105**, 1633
- Fynbo J. P. U., Ledoux C., Møller P., Thomsen B., Burud I., 2003, *A&A*, **407**, 147
- Fynbo J. P. U., Prochaska J. X., Sommer-Larsen J., Dessauges-Zavadsky M., Møller P., 2008, *ApJ*, **683**, 321
- Fynbo J. P. U., et al., 2011, *MNRAS*, **413**, 2481
- Fynbo J. P. U., et al., 2013, *MNRAS*, **436**, 361
- Geach J. E., Smail I., Moran S. M., MacArthur L. A., Lagos C. d. P., Edge A. C., 2011, *ApJ*, **730**, L19
- Geach J. E., et al., 2014, *Nature*, **516**, 68
- Ginolfi M., et al., 2017, *MNRAS*, **468**, 3468
- Kacprzak G. G., Murphy M. T., Churchill C. W., 2010, *MNRAS*, **406**, 445
- Kanekar N., et al., 2018, *ApJ*, **856**, L23
- Klitsch A., Péroux C., Zwaan M. A., Smail I., Oteo I., Biggs A. D., Popping G., Swinbank A. M., 2018, *MNRAS*, **475**, 492
- Ledoux C., Petitjean P., Bergeron J., Wampler E. J., Srianand R., 1998, *A&A*, **337**, 51
- Ledoux C., Petitjean P., Fynbo J. P. U., Møller P., Srianand R., 2006, *A&A*, **457**, 71
- Leroy A. K., et al., 2009, *AJ*, **137**, 4670
- Macchetto F., Lipari S., Gialalisco M., Turnshek D. A., Sparks W. B., 1993, *ApJ*, **404**, 511
- Magdis G. E., et al., 2012a, *ApJ*, **758**, L9
- Magdis G. E., et al., 2012b, *ApJ*, **760**, 6
- Magnelli B., et al., 2012, *A&A*, **548**, A22
- Mantz A. B., Allen S. W., Morris R. G., Simionescu A., Urban O., Werner N., Zhuravleva I., 2017, *MNRAS*, **472**, 2877
- McMullin J. P., Waters B., Schiebel D., Young W., Golap K., 2007, in Shaw R. A., Hill F., Bell D. J., eds, *Astronomical Society of the Pacific Conference Series Vol. 376, Astronomical Data Analysis Software and Systems XVI*. p. 127
- Møller P., Warren S. J., 1993, *A&A*, **270**, 43
- Møller P., Warren S. J., 1998, *MNRAS*, **299**, 661
- Møller P., Fynbo J. P. U., Ledoux C., Nilsson K. K., 2013, *MNRAS*, **430**, 2680
- Møller P., et al., 2018, *MNRAS*, **474**, 4039
- Neeleman M., Wolfe A. M., Prochaska J. X., Rafelski M., 2013, *ApJ*, **769**, 54
- Neeleman M., et al., 2016, *ApJ*, **820**, L39
- Neeleman M., Kanekar N., Prochaska J. X., Rafelski M., Carilli C. L., Wolfe A. M., 2017, *Science*, **355**, 1285
- Neeleman M., Kanekar N., Prochaska J. X., Christensen L., Dessauges-Zavadsky M., Fynbo J. P. U., Møller P., Zwaan M. A., 2018, *ApJ*, **856**, L12
- Planck Collaboration et al., 2016, *A&A*, **594**, A13
- Pontzen A., et al., 2008, *MNRAS*, **390**, 1349
- Prochaska J. X., Wolfe A. M., 1997, *ApJ*, **487**, 73
- Rahmani H., et al., 2018, *MNRAS*, **474**, 254
- Renzini A., 1997, *ApJ*, **488**, 35
- Riechers D. A., Carilli C. L., Walter F., Momjian E., 2010, *ApJ*, **724**, L153
- Schlafly E. F., Finkbeiner D. P., 2011, *ApJ*, **737**, 103
- Schulze S., et al., 2012, *A&A*, **546**, A20
- Solomon P. M., Vanden Bout P. A., 2005, *ARA&A*, **43**, 677
- Sommer-Larsen J., Fynbo J. P. U., 2017, *MNRAS*, **464**, 2441
- Steidel C. C., Erb D. K., Shapley A. E., Pettini M., Reddy N., Bogosavljević M., Rudie G. C., Rakic O., 2010, *ApJ*, **717**, 289
- Tacconi L. J., et al., 2010, *Nature*, **463**, 781
- Tacconi L. J., et al., 2013, *ApJ*, **768**, 74
- Walter F., Weiss A., Scoville N., 2002, *ApJ*, **580**, L21
- Warren S. J., Møller P., 1996, *A&A*, **311**, 25
- Wolfe A. M., Gawiser E., Prochaska J. X., 2005, *ARA&A*, **43**, 861
- da Cunha E., Charlot S., Elbaz D., 2008, *MNRAS*, **388**, 1595

This paper has been typeset from a $\text{\TeX}/\text{\LaTeX}$ file prepared by the author.